

ACTIVITY DIAGRAMS OF ZEOLITES: IMPLICATIONS FOR THE OCCURRENCES OF ZEOLITES IN TURKEY AND OF ERIONITE WORLDWIDE

REZAN BIRSOY*

Dokuz Eylül University, Engineering Faculty, Geology Department, 35100, Bornova, Izmir, Turkey

Abstract—Sedimentary zeolite occurrences are widespread in Central and Western Anatolia, Turkey. Erionite occurrences in Central Anatolia have significant health implications for inhabitants of the region. The widespread occurrences of zeolites are generally associated with volcano-sedimentary rocks and consist of low-temperature forms. The aim of the work was to define specifically the formation mechanism and chemical characteristics of these volcano-sedimentary deposits, and particularly, the stability conditions for erionite. The first step was to construct chemical potential diagrams and calculate thermodynamic data for erionite and Ca-saponite. Then, equilibrium activity diagrams were calculated for the zeolites and related minerals in the system of Ca-Na-K-Mg-Fe-Al-Si and H₂O. Stability diagrams for $\log [a_{\text{Ca}^{2+}}/(a_{\text{H}^+})^2] - \log [a_{\text{Na}^+}/a_{\text{H}^+}]$ and $\log [a_{\text{Ca}^{2+}}/(a_{\text{H}^+})^2] - \log [a_{\text{K}^+}/a_{\text{H}^+}]$ for various saturation phase activities of Al³⁺ and SiO_{2(aq)} were plotted for sedimentary conditions. The coexisting phases and chemical characteristics of the each deposit were evaluated by examination of the activity diagrams. Deposits which do not include some of the common sedimentary zeolites, possibly have high Al³⁺ activity (equal to or greater than gibbsite saturation) or low SiO_(aq) activity (less than quartz saturation) during formation. In addition, erionite was found to be very sensitive to the alkalinity of the system and is stable in only a limited range of thermochemical conditions.

Key Words—Activity-diagrams, Erionite, Turkey, Zeolites.

INTRODUCTION

Zeolites, more than most mineral groups, serve humans in various ways, as they have unique properties. The ancient civilizations of Anatolia used zeolites for many purposes. For the last three decades, however, zeolites have been considered dangerous, because of the cancerous effects of erionite found in Cappadocia (Ross *et al.*, 1993). Even though only erionite-bearing deposits are known carcinogens, all zeolite deposits appear to have been given that label. In fact, erionite is not widespread in nature suggesting limited conditions of formation. Thus, the stability conditions, occurrences and paragenetic relations of the zeolite group were examined in the present study with special emphasis on the formation of erionite.

The most common zeolite occurrences of Turkey, from central to western Anatolia, are in Beypazar (Gündoğdu *et al.*, 1985; Helvacı *et al.*, 1987; Schmitz, 1991), Yozgat (Yalçın *et al.*, 1997), Nevşehir (Cappadocia) (Temel and Gündoğdu, 1996), Kırka (Yalçın, 1988), Emet (Yalçın and Gündoğdu, 1985, 1987), Şile (Esenli *et al.*, 1997), Bigadiç (Gündoğdu, 1984; Sirkecioğlu *et al.* 1990; Gündoğdu *et al.* 1989), Gördes (Esenli and Özpeker, 1993; Esenli, 1993; Baykal, 1995) and Keşan (İçöz and Türkmenoğlu 1997) (Figure 1). The common zeolites and other minerals reported in Turkish deposits (Table 1) are clinoptilolite, erionite, chabazite, analcime, phillipsite, mordenite,

smectite, quartz, opal-CT and K-feldspar in Nevşehir, clinoptilolite and smectite in Yozgat, and analcime, clinoptilolite, phillipsite, K-feldspar, smectite, quartz and calcite in Beypazar. The Bigadiç deposit consists of clinoptilolite, heulandite, analcime, phillipsite, smectite, opal-CT, quartz, K-feldspar and calcite. Kırka is characterized by clinoptilolite, heulandite and minor amounts of analcime, calcite, opal-CT, K-feldspar, smectite and quartz. Clinoptilolite, analcime, opal-CT, K-feldspar, smectite, quartz and calcite are typical of the Emet deposits. Clinoptilolite, heulandite, opal-CT, quartz and smectite are found in the Gördes deposits; analcime, clinoptilolite, smectite, quartz, cristobalite and calcite in the Keşan area; and mordenite, K-feldspar, opal-CT and quartz in the Şile deposit.

The zeolites in Turkey are associated with clay minerals, borates, carbonates and soda minerals (mainly trona and in rare instances, nahcolite). They are also found in close association with lignite-bearing lacustrine rocks and evaporates. For example, the zeolite minerals are found with soda minerals, clays and carbonates in association with coal deposits in the Beypazar region, whereas they are found with borates, carbonates and clays in the Kırka, Emet and Bigadiç areas. In the Gördes and Yozgat regions, zeolites coexist with carbonate and clay minerals and they are interbedded with coal horizons. In all of these occurrences, except that located in the Şile area, the sedimentary rock successions including zeolite minerals, are closely associated with successions of volcanogenic tuffs and they were deposited in lacustrine environments. In this study only those zeolite occurrences in Turkey, on which

* E-mail address of corresponding author:
rezan.birsoy@deu.edu.tr

Table 1. Mineral assemblages of Turkish deposits.

Deposits	Associated minerals
Beypazarı	Clinoptilolite, analcime, saponite, K-feldspar, smectite, quartz, calcite
Yozgat	Clinoptilolite, smectite
Nevşehir (Cappadocia)	Erionite, chabazite, analcime, phillipsite, mordenite ± clinoptilolite, smectite, quartz, opal-CT, K-feldspar
Kırka	Clinoptilolite, heulandite, analcime, calcite, opal-CT, smectite, K-feldspar, quartz
Emet	Clinoptilolite, analcime, opal-CT, K-feldspar, smectite, quartz, calcite
Şile	Mordenite, K-feldspar, opal-CT, quartz
Bigadiç	Clinoptilolite, heulandite, analcime, phillipsite, smectite, opal-CT, quartz, K-feldspar
Gördes	Clinoptilolite, heulandite, opal-CT, quartz, smectite
Keşan	Analcime, clinoptilolite, smectite, quartz, cristobalite, calcite

in-depth studies had been performed, and for which detailed information was available, are considered.

The paragenetic assemblages of these various deposits show some interesting characteristics. In two similar deposits, for example, one may include zeolite minerals with clay minerals (smectite and sepiolite) and the other, no zeolites. In addition, some zeolite occurrences have clinoptilolite with or without analcime (Kırka, Emet, Bigadiç, Yozgat, Beypazarı and Keşan). In Kırka and Beypazarı, clinoptilolite is found with phillipsite. Erionite, chabazite, analcime with or without mordenite and clinoptilolite are the mineralogical assemblages of Cappadocia. In Şile, mordenite is the only zeolitic mineral present.

It is well known that the presence or absence of zeolite minerals and types of zeolitic minerals in a deposit depends on activities of Ca, Na, K, Mg Al, SiO_2 (aq), H^+ (pH) ions and temperature of the system. However, the influence of these parameters have not been quantified, especially, formation conditions for erionite. Most of the volcano-sedimentary erionites in the world, other than those in Turkey are located in the USA and in a few locations in Tanzania, Kenya and Georgia (Gude and Sheppard, 1981). Several investigators have studied the factors that may control the stabilities of zeolites, specifically on the zeolites of Yucca Mountain (Bowers and Burns, 1990; Chipera and Bish, 1997), but none of these studies considered the

stabilities of erionite. Consequently, the present study for various chemical environments has been undertaken to define the stability limits of the zeolitic occurrences.

DATA AND METHODS

Much of the data used to calculate the stability diagrams of zeolites and related minerals are tabulated and found in Tardy and Garrels (1974), Nriagu (1975), Robie *et al.* (1978), Helgeson *et al.* (1978), Johnson *et al.* (1983), Bowers *et al.* (1984) and Bowers and Burns (1990). All these tables have the same origin and the data are consistent. For two minerals of interest in this study, no Gibbs free energy of formation data (ΔG_f^0) are available, namely erionite and Ca-saponite at 25°C. In such cases, various methods can be applied to estimate the unknown data (Tardy and Garrels, 1974; Chen, 1975; Nriagu, 1975; Iglasia and Aznar, 1984). In the present study, the methods of Chen (1975), Nriagu (1975) and Iglasia and Aznar (1984), which are similar in approach, were used and tested for the precision of the estimated value for similar structural types. In order to verify the consistency of the data from the works of different authors, the free energies of minerals which were already known, were recalculated and checked. Values of ΔG_f^0 used in this study are shown in Table 2. The minerals in the table were selected because they coexist in Turkish deposits and are also compositionally related

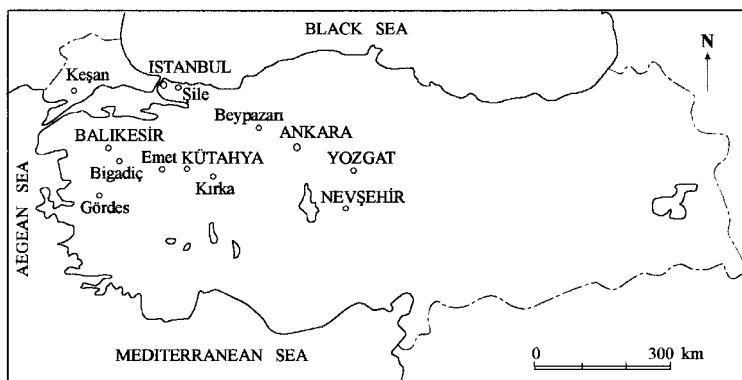


Figure 1. Locations of zeolite occurrences in Turkey.

Table 2. Minerals, formulae and free energies (modified after Bowers and Burns, 1990).

Mineral name	Formula	$\Delta G_f^0(298)$ kJ/mol
Quartz	SiO ₂	-856.239 ¹
Amorphous silica	SiO ₂	-850.599 ¹
Gibbsite	Al(OH) ₃	-1158.800 ²
Kaolinite	Al ₂ Si ₂ O ₅ (OH) ₄	-3781.499 ²
Pyrophyllite	Al ₂ Si ₄ O ₁₀ (OH) ₂	-5250.920 ³
Wollastonite	CaSiO ₃	-1545.758 ³
Anorthite	CaAl ₂ Si ₂ O ₈	-3992.783 ³
Grossular	Ca ₃ Al ₂ Si ₃ O ₁₂	-6263.309 ³
Gehlenite	Ca ₂ Al ₂ SiO ₇	-3780.612 ³
Prehnite	Ca ₂ Al ₂ Si ₃ O ₁₀ (OH) ₂	-5818.007 ³
Laumontite	CaAl ₂ Si ₄ O ₁₂ ·4H ₂ O	-6682.028 ³
Chabazite	CaAl ₂ Si ₄ O ₁₂ ·6H ₂ O	-7165.673 ⁴
Scolecite	CaAl ₂ Si ₃ O ₁₀ ·3H ₂ O	-5597.999 ⁵
Heulandite	CaAl ₂ Si ₇ O ₁₈ ·6H ₂ O	-9734.389 ⁴
Albite	NaAlSi ₃ O ₈	-3708.313 ³
Nepheline	NaAlSiO ₄	-1978.496 ¹
Paragonite	NaAl ₂ (AlSi ₃ O ₁₀)(OH) ₂	-5548.034 ³
Analcime	NaAlSi ₂ O ₆ ·H ₂ O	-3088.202 ¹
Natrolite	Na ₂ Al ₂ Si ₃ O ₁₀ ·2H ₂ O	-5316.692 ⁵
Mordenite	NaAlSi ₅ O ₁₂ ·3H ₂ O	-6132.267 ⁴
K-feldspar	KAlSi ₃ O ₈	-3746.245 ¹
Kalsilite	KAlSiO ₄	-2015.642 ³
Muscovite	KAl ₂ (AlSi ₃ O ₁₀)(OH) ₂	-5591.083 ³
K-phillipsite	K ₂ Al ₂ Si ₅ O ₁₄ ·5H ₂ O	-7830.189 ⁴
Phillipsite	Na _{1.08} K _{0.80} Al _{1.88} Si _{6.12} O ₁₆ ·6H ₂ O	-8840.169 ⁴
Stilbite	NaCa ₂ Al ₅ Si ₁₃ O ₃₆ ·14H ₂ O	-20223.661 ⁴
Mesolite	Na _{0.676} Ca _{0.657} Al _{1.99} Si _{3.01} O ₁₀ ·2.647H ₂ O	-5513.294 ⁵
Clinoptilolite	Na _{0.56} K _{0.98} Ca _{1.5} Mg _{1.23} Al _{6.7} Fe _{0.3} Si ₂₉ O ₇₂ ·22H ₂ O	-37897.789 ⁴
Erionite	CaK ₃ Na ₃ Al ₈ Si ₂₈ O ₇₂ ·27H ₂ O	-39614.769 ⁶
Ca-saponite	Ca _{0.165} Mg ₃ (Al _{0.33} Si _{3.67} O ₁₀)(OH) ₂	-5600.092 ⁶
Hematite	Fe ₂ O ₃	-743.622 ¹
Calcite	CaCO ₃	-1130.098 ³
Dolomite	CaMg(CO ₃) ₂	-2167.228 ³

¹ Robie *et al.* (1978)² Tardy and Garrels (1974)³ Helgeson *et al.* (1978)⁴ Bowers and Burns (1990)⁵ Johnson *et al.* (1983)⁶ Present study

to zeolites. Furthermore, some minerals were assumed as saturation phases and were used as the reference for the activity ratios of some cations, *e.g.* Ca-saponite (tri-octahedral smectite), hematite, amorphous silica + pyrophyllite (*cf.* dioctahedral smectite). The method for calculating activity diagrams can be seen elsewhere (Garrels and Christ, 1965; Bowers *et al.*, 1984). It is well known that zeolites may have significant variations in their chemical compositions. Even within the same deposit, the chemical composition of a particular zeolite species may change vertically and horizontally. In the present study, the exact chemical compositions of the zeolites in the Turkish deposits were not used; instead ideal formulae for the minerals were employed. In this case, the general appearance and phase relations of the diagrams do not change but the size and shape of the stability area may alter. However this does not affect the interpretations and the applications of diagrams.

Bowers and Burns (1990) also calculated activity diagrams for zeolite minerals occurring at Yucca Mountain, Nevada. These diagrams might have been used to interpret the mineral assemblages of Turkish deposits, but there were positional and slope displacements of some of the mineral phases on the activity diagrams (*e.g.* the slope between mesolite and phillipsite should not be negative on Figures 8b and 8c in the Bowers and Burns (1990) paper). Also, erionite was not considered, even though it is present to a limited extent in the Yucca Mountain deposits (Bish and Chipera, 1991). Therefore, in order to see the compositional control and general pattern of the activity diagrams, schematic chemical potential diagrams were constructed (Figures 2 and 3) by geometric procedures described by Korzhinski (1959). The activity diagrams of the zeolite and related minerals were then calculated with the guidance of these chemical potential diagrams in the

system Ca-Na-K-Mg-Fe-Al-Si and H₂O. In such systems, the boundary conditions need to be defined in order to construct the orthogonal activity diagrams. In the present study, $\log [a_{\text{Ca}^{2+}}/(a_{\text{H}^+})^2] - \log [a_{\text{Na}^+}/a_{\text{H}^+}]$ and $\log [a_{\text{Ca}^{2+}}/(a_{\text{H}^+})^2] - \log [a_{\text{K}^+}/a_{\text{H}^+}]$ are chosen as dependent and independent variables, respectively. In all the reactions, the activity of H₂O is fixed as unity. All mineral pairs were balanced with respect to Al³⁺ and also to SiO_{2(aq)}, eliminating one variable each time, and assigning fixed value to the others. With mineral pairs balanced with respect to SiO_{2(aq)} and saturation phases chosen as gibbsite, pyrophyllite + kaolinite, pyrophyllite + amorphous silica and 4.5 (arbitrary low Al activity) provides $\log [a_{\text{Al}^{3+}}/(a_{\text{H}^+})^3]$ values. After the elimination of the Al³⁺, the $\log [a_{\text{SiO}_2(\text{aq})}]$ value was assigned as saturation phases of SiO_{2(am)} amorphous silica, pyrophyllite + kaolinite and quartz. The other saturation phases are hematite for $\log [a_{\text{Fe}^{3+}}/(a_{\text{H}^+})^3]$, saponite for $\log [a_{\text{Mg}^{2+}}/(a_{\text{H}^+})^2]$, K-feldspar for $\log [a_{\text{K}^+}/a_{\text{H}^+}]$, albite for $\log [a_{\text{Na}^+}/a_{\text{H}^+}]$ and calcite for $\log [a_{\text{Ca}^{2+}}/(a_{\text{H}^+})^2]$. On all

activity diagrams, the stability lines of calcite and dolomite are indicated with dashed lines.

RESULTS

Chemical potential diagrams

Figures 2a and 2b show compositional relations in the system CaO-Na₂O-Al₂O₃-SiO₂-H₂O and CaO-K₂O-Al₂O₃-SiO₂-H₂O by conserving Al₂O₃ for the phases that occur with zeolite minerals. Figures 3a and 3b illustrate the general relationships at the same systems given above except by the conservation of the SiO₂. Correlation of Figures 2a with 3a and 2b with 3b reveals that by assuming Al or Si to be inert components causes different stability assemblages. Therefore, in order to construct the activity diagrams, all equilibrium reactions were calculated by balancing with respect to both Al and Si.

Activity diagrams

Figures 4 and 5 are activity diagrams for the system Ca-Na-K-Al-Si-H₂O balanced with respect to Al. Values

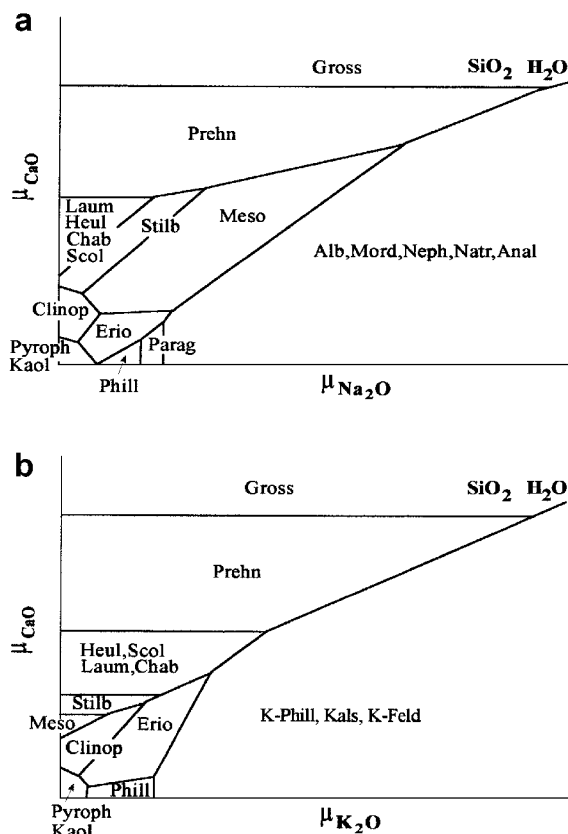


Figure 2. Schematic chemical potential diagrams in the presence of SiO₂ and H₂O with respect to components (a) CaO and Na₂O, (b) CaO and K₂O. Alb: albite; Anal: analcime; Chab: chabazite; Clinop: clinoptilolite; Erio: erionite; Gross: grossular; Heul: heulandite; Kals: kalsilite; Kaol: kaolinite; K-feld: K-feldspar; K-phill: K-phillipsite; Laum: laumontite; Meso: mesolite; Mord: mordenite; Natr: natrolite; Parag: paragonite; Phill: phillipsite; Prehn: prehnite; Pyroph: pyrophyllite; Scol: scolecite; Stilb: stilbite.

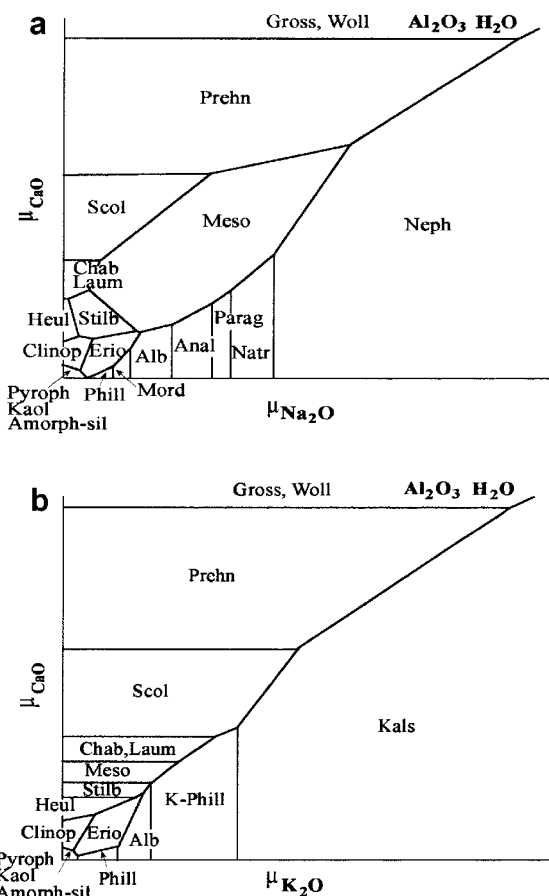


Figure 3. Schematic chemical potential diagrams in the presence of Al₂O₃ and H₂O with respect to components (a) CaO and Na₂O, and (b) CaO and K₂O. Abbreviations as in Figure 2; Amorph-sil: amorphous silica.

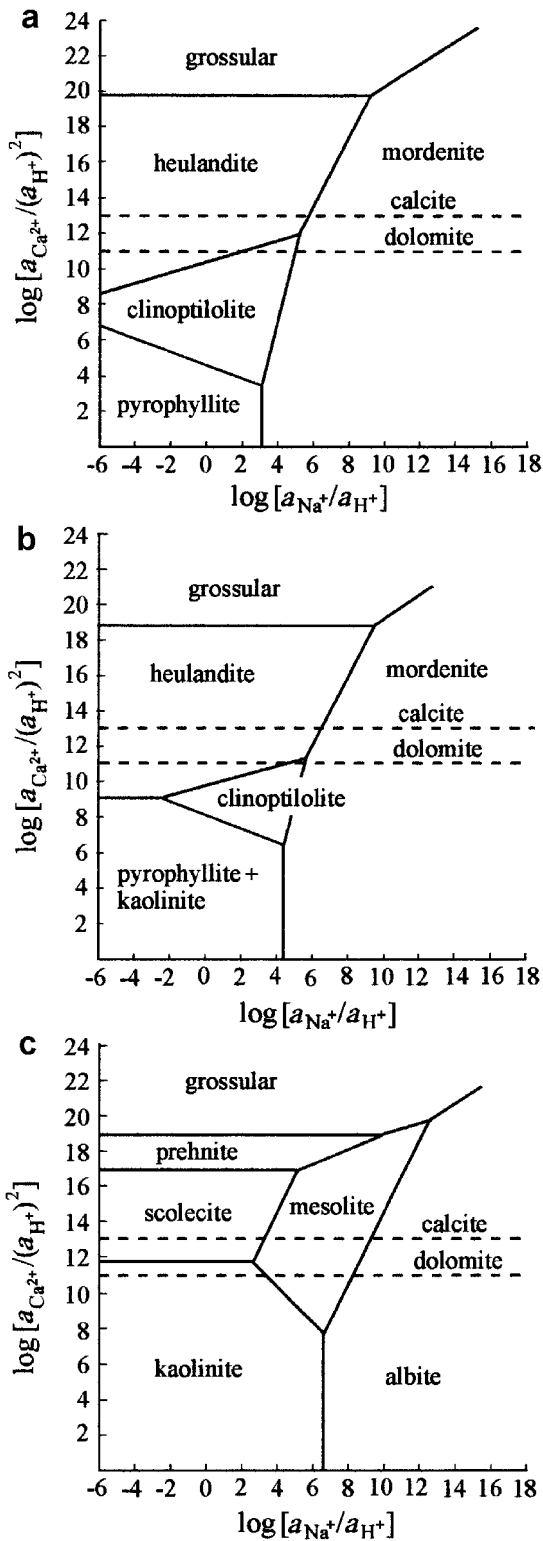


Figure 4. Activity diagrams for the system Ca-Na-K-Al-Si-H₂O balanced with respect to Al for different silica activities at 25°C for (a) amorphous silica, (b) pyrophyllite + kaolinite, and (c) quartz. In addition, K-feldspar, hematite and Ca-saponite are also saturation phases.

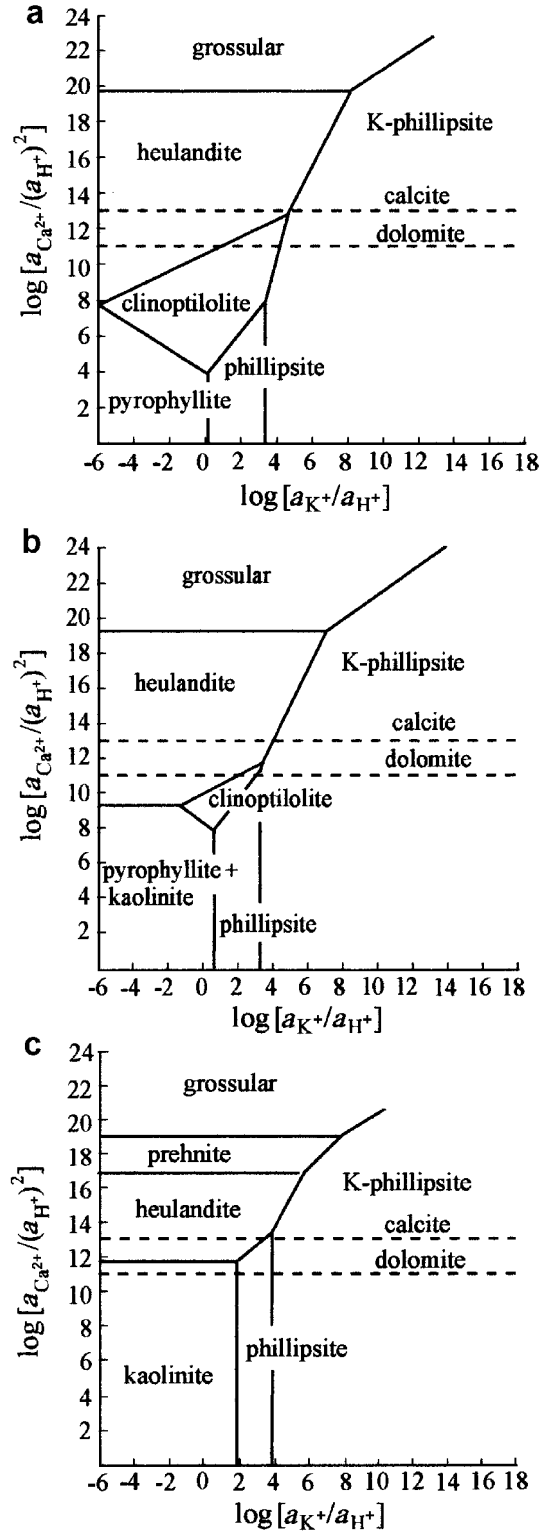


Figure 5. Activity diagrams for the system Ca-Na-K-Al-Si-H₂O balanced with respect to Al for different silica activities at 25°C for (a) amorphous silica, (b) pyrophyllite + kaolinite, and (c) quartz. In addition, albite, hematite and Ca-saponite are also saturation phases.

of $\log [a_{\text{Ca}^{2+}}/(a_{\text{H}^+})^2] - \log [a_{\text{Na}^+}/a_{\text{H}^+}]$ are plotted on Figure 4a–c and $\log [a_{\text{Ca}^{2+}}/(a_{\text{H}^+})^2] - \log [a_{\text{K}^+}/a_{\text{H}^+}]$ on Figure 5a–c. Both series illustrate the decreasing values of $\log [a_{\text{SiO}_2}]$ as amorphous silica, pyrophyllite + kaolinite and quartz, respectively. Comparison of the activity diagrams in Figures 4 and 5 through different activities of Si reveals that decreasing the silica activity affects the size of the stability field and the occurrence of some zeolite minerals. In Figure 4, for example, the stability fields of clinoptilolite, heulandite and mordenite decrease with decreasing silica and stability fields form for scolecite, mesolite and kaolinite when the system is saturated with respect to quartz. Figure 5 for K-bearing zeolite minerals is very similar to the Na counterparts in Figure 4, except that heulandite, phillipsite and K-phillipsite persist even at quartz saturation.

The effects of the various Al activities can be observed for the Ca–Na–K–Al–Si–H₂O system in Figures 6 and 7. The system was balanced with respect to Si, and four Al activities were considered; low arbitrary Al activity (4.5), and saturation limits of amorphous silica + pyrophyllite, pyrophyllite + kaolinite and gibbsite, in increasing order. Comparison of the

activity diagrams shown in Figures 6 and 7 indicates that different Al activities do not represent a linear trend as observed in Figures 4 and 5. The influence of the activity of Al on the stabilities of zeolites are much more complicated than expected. The most suitable Al saturation is amorphous silica + pyrophyllite which accounts for the coexistence of smectites with zeolites in Turkish deposits. In the most of the deposits, quartz and cristobalite are also present as silica phases. When the quartz was plotted instead of amorphous silica, it covered a larger area than amorphous silica. In this case, some of these diagrams would not contain clinoptilolite as a stable phase.

In Figure 6a–d, the stability field of clinoptilolite increases up to amorphous silica + pyrophyllite saturation limits then decreases and vanishes at gibbsite saturation. Heulandite also exhibits a similar trend with clinoptilolite. In contrast, both mordenite and analcime have a decreasing linear trend and vanish at the stability of gibbsite. This probably resulted from the activities of dissolved Al species in equilibrium with amorphous silica + pyrophyllite, pyrophyllite + kaolinite and gibbsite in the solution (Wesolowski and Palmer, 1994).

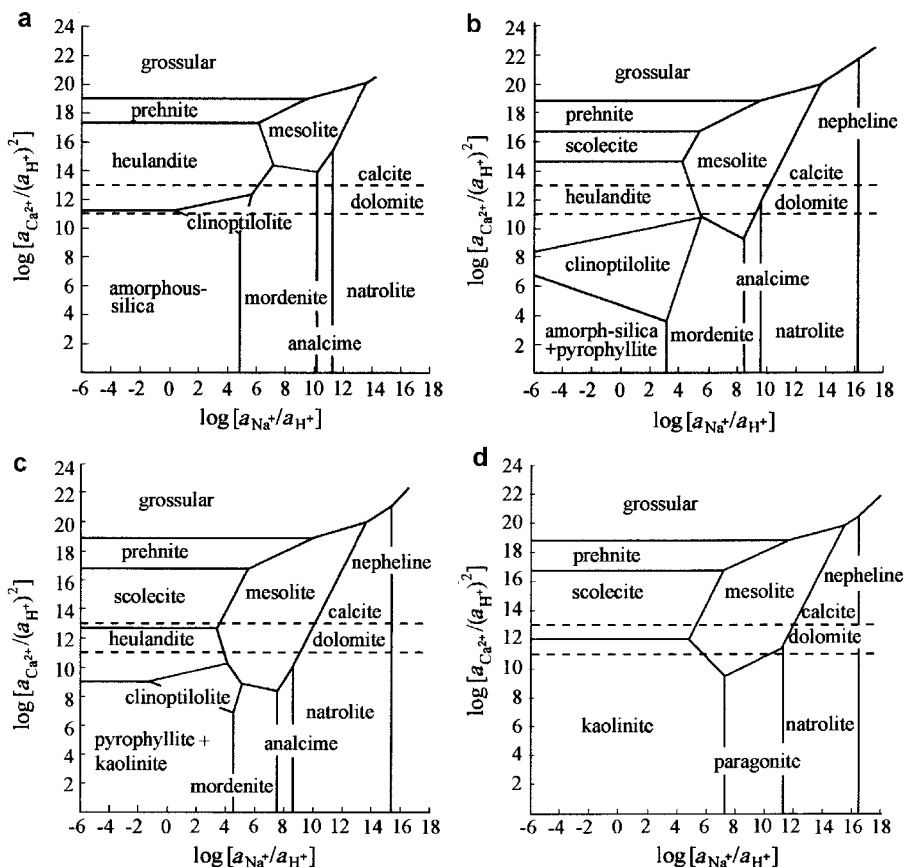


Figure 6. Activity diagrams for the system Ca–Na–K–Al–Si–H₂O balanced with respect to Si for different Al activities at 25°C for (a) low Al activity ($\log [a_{\text{Al}^{3+}}/(a_{\text{H}^+})^3] = 4.5$), (b) pyrophyllite + amorphous silica, (c) pyrophyllite + kaolinite, and (d) gibbsite. K-feldspar, hematite and Ca-saponite are additional saturation phases.

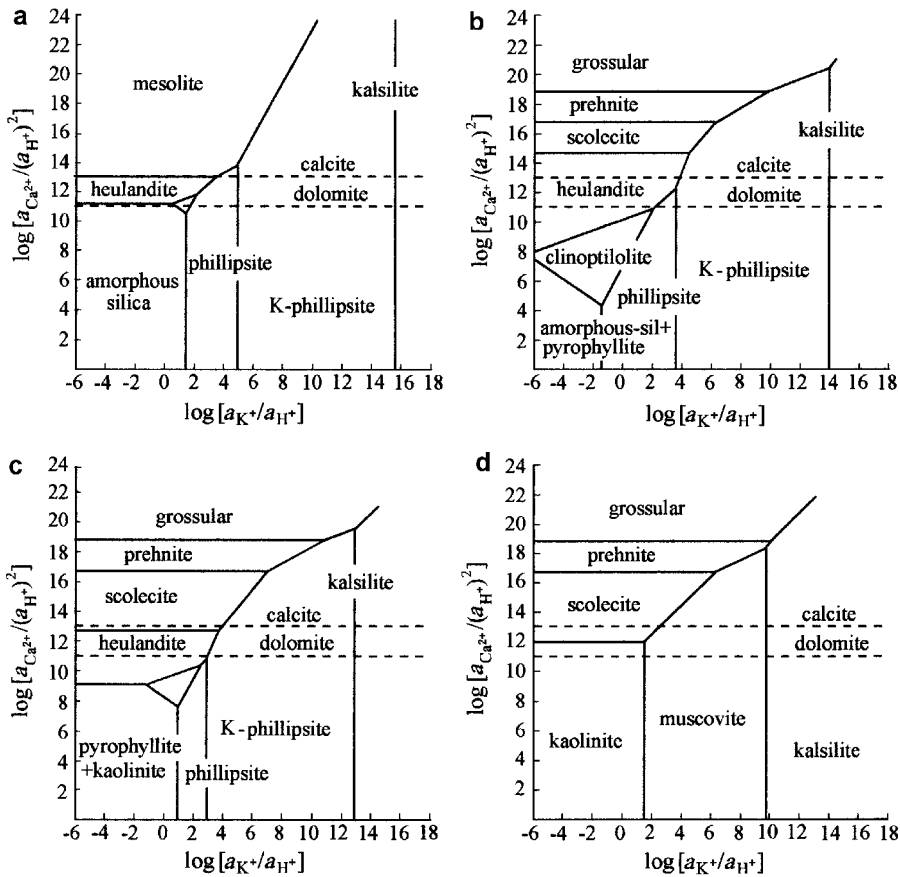


Figure 7. Activity diagrams for the system Ca-Na-K-Al-Si-H₂O balanced with respect to Si at 25°C for (a) low Al activity ($\log [a_{Al^{3+}}/(a_{H^+})^3] = 4.5$), (b) pyrophyllite + amorphous silica, (c) pyrophyllite+kaolinite, and (d) gibbsite. Albite, hematite and Ca-saponite are additional saturation phases.

In Figure 7a–d, clinoptilolite, heulandite and scolecite at corresponding activities of Al behave the same as in the Figure 6. Mordenite, analcime and natrolite are replaced by K counterparts, namely phillipsite, K-phillipsite and kalsilite. Mesolite, however, does not persist as in Figure 6 up to gibbsite saturation. In fact it is stable only at low Al activity (Figure 7a).

It is also noted that erionite does not appear on any of the activity diagrams. After performing various tests with increasing or decreasing Na and K activities, the stabilization of erionite can be attained (Figure 8). The conditions that allow the stabilization of erionite seem to be very limited, thus explaining why occurrences are so rare.

DISCUSSION

The activity diagrams illustrate that the formation of the various zeolite minerals and related minerals are affected most by SiO₂ and Al activities. The solubility of SiO₂ and dissolved Al species at 25°C are certainly controlled by pH (Wesolowski and Palmer, 1994), which is controlled by carbonate equilibria in natural aqueous systems (Garrels and Christ, 1965).

Activity diagrams were constructed by the elimination of the Al ion illustrated in Figures 4 and 5, which are the same as in Bowers and Burns (1990). As the silica activity decreases, the stability field of the

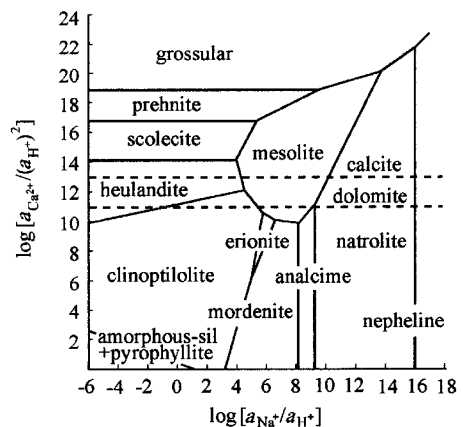


Figure 8. Activity diagrams for the system Ca-Na-K-Al-Si-H₂O balanced with respect to Si at 25°C for medium Al activity ($\log [a_{Al^{3+}}/(a_{H^+})^3] = 6.5$) and high K activity ($\log [a_{K^+}/a_{H^+}] = 7$). Hematite and Ca-saponite are additional saturation phases.

clinoptilolite and heulandite also decreases. Only heulandite can persist at quartz saturation. At quartz saturation, albite and kaolinite become stable phases. Şile-type zeolite and clay occurrence is well demonstrated in Figure 4a,b. Mordenite, kaolinite, K-feldspar and the smectite, as coexisting phases (Esenli *et al.*, 1997), can be stable in a range of silica activities lower than that for amorphous silica saturation and greater than that for cristobalite saturation as seen in Figure 4b.

The assemblage at Kırka (Yalçın *et al.*, 1989) and part of that at Gördes (Esenli and Özpeker, 1993) can be represented by Figures 5a and b. The activity relations of zeolites and related minerals, given the presence or absence of carbonate minerals, can be evaluated for the Kırka deposit.

Figure 6 in this work is the same as Figure 8 in Bowers and Burns (1990) with some minor differences. The stability boundary slope between phillipsite and mesolite is shown as positive in Figure 8 of Bowers and Burns (1990), but when the equilibrium equation between mesolite and phillipsite is examined it is clear that the slope is negative and not positive. This study was conducted because some other differences were also expected between the diagrams of Bowers and Burns (1990) and the present study. It transpired that analcime instead of phillipsite is stable in the diagram. The other differences may result for similar reasons. The size differences of the stability fields possibly resulted from the variations in cation activities, used in the present study.

The most common zeolite in all Turkish deposits is clinoptilolite, which is favored by the Al activity $\log [a_{\text{Al}^{3+}}/(a_{\text{H}^+})^3]$ being >4 and less than the gibbsite saturation. The maximum stability field can be observed at the amorphous silica + pyrophyllite (compositionally equivalent to smectite) saturation value of $\log [a_{\text{Al}^{3+}}/(a_{\text{H}^+})^3]$ (Figures 6a,b; 7a,b). K-feldspar is also a saturation phase at a value of $\log [a_{\text{K}^+}/a_{\text{H}^+}]$. This is the most favorable condition for clinoptilolite, heulandite, phillipsite, smectite, K-feldspar and silica phases (other than quartz). It means that this condition is consistent with many of the zeolite assemblages of Turkey such as Bepazan, Bigadiç, Kırka, Emet and some parts of Gördes. Chemical potential diagrams with the activity diagrams of Figures 6 and 7 in which the silica was inert, indicate that the conditions never reached the stability limits of mesolite, scolecite and mordenite. Figure 7 shows zeolite-forming basins with no Na-rich plagioclase. Calcite is in equilibrium with mordenite, heulandite and analcime. In all of these deposits, diagenetic evolution of mineral assemblages, horizontally from onshore to offshore and vertically, follows the path of increasing activity values of cations and pH, and is consistent with the activity diagrams. Many observed and/or suggested formation models can easily be demonstrated on these activity diagrams.

Bowers and Burns (1990) did not consider erionite as a phase in their calculations. Even though erionite was

included in the present study, it did not appear on any diagrams in the conditions listed above. Inspection of the diagrams indicates that clinoptilolite, heulandite, mordenite and phillipsite are favored at the highest silica, and lowest Na and K activities when the system is balanced with respect to Al. On the contrary, when the system is balanced with respect to silica, clinoptilolite, heulandite, mordenite and phillipsite are favored at moderate alumina and Na, and lowest K activities. Erionite is not present in either case as an equilibrium phase. To determine favorable conditions for erionite, a series of experiments was run in order to construct chemical potential diagrams. Equilibria between erionite and clinoptilolite and mordenite were achieved at moderate Al and very high K activities (Figure 8). When the erionite-containing volcano-sedimentary deposits of the western United States (Yucca Mountain, Chalk Hill), Tanzania (Lake Natron), Kenya (Lake Magadi) and Turkey (Cappadocia) are compared, it can be seen that all have common properties such as similar starting material, and are rich in alkali content (Hay, 1978; Surdam and Sheppard, 1978; Gude and Sheppard, 1981). This alkali content can be provided by the host rock or by the solution during the formation of erionite. Interpretations by Sheppard (1989, 1991) indicated that the formation of erionite requires, high alkali content and pH which, is in agreement with the present study.

CONCLUSIONS

The activity diagrams presented in this study compare well with field data and provide some interpretations about the stabilities of the zeolite and related minerals. It has been calculated quantitatively that silica and Al concentrations, which are controlled by pH, are the main variables for zeolite formation. Thus, silica activity should be greater than quartz saturation and Al activity less than gibbsite saturation, for the formation of the observed zeolites. Most of the calculated activity diagrams are representative of the Turkish zeolite occurrences. For the formation of erionite, however, besides the significance of silica and Al, the alkali content and alkalinity of the solution are very determinative. For example, the coexistence of clinoptilolite and erionite needs to have twice as much K as K-feldspar saturation. This condition can probably be provided during burial diagenetic reactions. For the ongoing activity calculations of zeolites, the stability limits of various compositions of erionite and clinoptilolite will be tested.

ACKNOWLEDGMENTS

Helpful comments by Dr M. Gunter and an anonymous reviewer are appreciated.

REFERENCES

- Baykal, A. (1995) Güneşli (Gördes) zeolitli Neojen serilerinin kil mineralojisi. Pp. 141–143 in: *VII Ulusal Kil*

- Semposyumu, Bildiriler Kitabı*, Turkey.
- Bish, D.L. and Chipera, S. (1991) Detection of trace amount of erionite using X-ray powder diffraction: Erionite in tuffs of Yucca Mountain, Nevada and Central Turkey. *Clays and Clay Minerals*, **39**, 437–445.
- Bowers, T.S. and Burns, R.G. (1990) Activity diagrams for clinoptilolite: Susceptibility of this zeolite to further diagenetic reactions. *American Mineralogist*, **75**, 601–619.
- Bowers, T.S., Jackson, K.J. and Helgeson, H.C. (1984) *Equilibrium Activity Diagrams*. Springer-Verlag, 397 pp.
- Chen, C.H. (1975) A method for estimation of standard free energies of formation of silicate minerals at 298.15 K. *American Journal of Science*, **275**, 801–817.
- Chipera, S. and Bish, D.L. (1997) Equilibrium modeling of clinoptilolite-analcime equilibria at Yucca Mountain, Nevada, USA. *Clays and Clay Minerals*, **45**, 226–239.
- Esenli, F. (1993) The chemical changes during zeolitization (Heulandite-Clinoptilolite type) of the acidic tuffs in the Gördes Neogene Basin. *Geological Bulletin of Turkey*, **6**, 37–44.
- Esenli, F. and Özpeker, I. (1993) Zeolitic diagenesis of Neogene basin and the mineralogy of Heulandite-Clinoptilolite around Gördes. *Geological Bulletin of Turkey*, **8**, 1–18.
- Esenli, F., Uz, B. and Kumbasar, I. (1997) Mordenite type zeolite occurrence in the Upper Cretaceous volcanics of Şile region, Istanbul-Turkey. *Geological Bulletin of Turkey*, **40**, 43–49.
- Garrels, R.M. and Christ, C.L. (1965) *Solutions, Minerals and Equilibria*. Harper and Row, New York, USA, 450 pp.
- Gude, A.J., 3rd and Sheppard, R.A. (1981) Woolly erionite from the Reese River zeolite deposit, Lander County, Nevada, and its relationship to other erionites. *Clays and Clay Minerals*, **29**, 378–384.
- Gündoğdu, M.N. (1984) Bigadiç gölsel baseninin jeolojisi. *Yerbilimleri*, **11**, 91–104.
- Gündoğdu, M.N., Bonnot-Coutois, C. and Clauer, N. (1989) Isotopic and chemical signatures of sedimentary smectite and diagenetic clinoptilolite of lacustrine Neogene basin near Bigadiç, Western Turkey. *Applied Geochemistry*, **4**, 635–644.
- Gündoğdu, M.N., Tenekeci, Ö., Öner, F., Dündar, A. and Kayakıran, S. (1985) Clay mineralogy of Beypazarı Trona deposits: Preliminary results. Pp. 141–143 in: *Proceedings of the 2nd Turkish National Clay Symposium*. Hacettepe University, Ankara, Turkey.
- Hay, R.L. (1978) Geologic occurrence of zeolites. Pp. 135–143 in: *Natural Zeolites, Occurrence, Properties, Use* (L.B. Sand and F.A. Mumpton, editors). Pergamon Press, New York, USA.
- Helgeson, H.C., Delany, J.M., Nesbitt, H.W. and Bird, D.K. (1978) Summary and critique of the thermodynamic properties of rock-forming minerals. *American Journal of Science*, **278-A**, 229 pp.
- Helvacı, C., İnci, U. and Yılmaz, H. (1987) Geology and Neogene trona deposits of the Beypazarı region, Turkey. *Doğa Mühendislik ve Çevre Dergisi*, **13**, 245–256.
- İçöz, S. and Türkmenoğlu, A. (1997) Mineralogical, petrographical and geochemical investigation of Eocene-Oligocene clastics from Keşan region, related to their origins, Thrace. Pp. 37–49 in: *Proceedings of the VIII National Clay Symposium, Kütahya*, Turkey.
- Johnson, G.K., Flotow, H.E., O'Hare, P.A.G. and Wise, W.S. (1983) Thermodynamic studies of zeolites: natrolite, mesolite and scolecite. *American Mineralogist*, **68**, 1134–1145.
- Korzinskii, D.S. (1959) *Physicochemical Basis of the Analysis of the Paragenesis of Minerals*. Chapman & Hall, London, 142 pp.
- La Iglasia, A. and Aznar, A.J. (1984) A method estimating the Gibbs energies of formation of zeolites. *Zeolites*, **6**, 26–29.
- Nriagu, J.O. (1975) Thermochemical approximations for clay minerals. *American Mineralogist*, **60**, 834–839.
- Robie, R.A., Hemingway, B.S. and Fisher, J.R. (1978) Thermodynamic properties of minerals and related substances at 298.15 K and 1 bar (10^5 pascals) pressure and at higher temperatures. *United State Geological Survey Bulletin*, **1452**, pp. 456.
- Ross, M., Nolan, R.P., Langer, A.M. and Cooper, W.C. (1993) Health effects of mineral dusts other than asbestos. Pp. 361–407 in: *Health Effects of Mineral Dusts* (G.D. Guthrie, Jr. and B.T. Mossman, editors). Reviews in Mineralogy, **28**. Mineralogical Society of America, Washington, D.C.
- Schmitz, H.-H. (1991) Ölschiefer des Miozäns in der Türkei – eine außergewöhnliche Genese in Zentralanatolien. *Geologisches Jahrbuch*, **A127**, 365–390.
- Sheppard, R.A. (1989) Zeolitic alteration of zeolitic tuffs, Western Snake River Plain, Idaho, USA. Pp. 501–510 in: *Zeolites: Facts, Figures, Future* (P.A. Jacobs and R.A. Van Santen, editors). Elsevier Science Publishers, Amsterdam, The Netherlands.
- Sheppard, R.A. (1991) Zeolitic diagenesis of tuffs in the Miocene Chalk Hills formation, Western Snake River Plain, Idaho. *United State Geological Survey Bulletin*, **1963**, 27 pp.
- Sirkecioglu, A., Esenli, F., Kumbasar, I., Eren, R.H. and Şenatalar, E.A. (1990) Mineralogical and chemical properties of Bigadiç clinoptilolite. Pp. 291–302 in: *International Earth Sciences Congress on Aegean Regions (IESCA 1990) V I* (M.Y. Savaşçın and A.H. Eronat, editors).
- Surdam, R.C. and Sheppard, R.A. (1978) Zeolites in saline, alkaline-lake deposits. Pp. 145–174 in: *Natural Zeolites, Occurrence, Properties, Use* (L.B. Sand and F.A. Mumpton, editors). Pergamon Press, New York, USA.
- Tardy, Y. and Garrels, R.M. (1974) A method of estimating the Gibbs energies of formation of layer silicates. *Geochimica et Cosmochimica Acta*, **38**, 1101–1116.
- Temel, A. and Gündoğdu, M.N. (1996) Zeolite occurrences and the erionite-mesothelioma relationship in Cappadocia, central Anatolia, Turkey. *Mineralium Deposita*, **31**, 539–547.
- Yalçın, H. (1988) *Kırka (Eskişehir) yöresi volkano-sedimentar oluşumlarının mineralojik-petrografik ve jeokimyasal incelenmesi*. PhD thesis, Hacettepe Üniversitesi, Ankara, 209 pp.
- Yalçın, H. and Gündoğdu, M. N. (1985) Emet gölsel Neojen baseninin kil mineralojisi Pp. 155–170 in: *II Ulusal Kil Sempozyumu Bildirileri* (M.N. Gündoğdu and H. Aksoy, editors). Hacettepe Üniversitesi, Ankara, Turkey.
- Yalçın, H. and Gündoğdu, M.N. (1987) Neojen yaşlı Emet gölsel volkansedimenter baseninin mineralojik-petrografik incelenmesi: Neoformasyon minerallerinin oluşumu ve dağılımı. *Yerbilimleri*, **14**, 45–61.
- Yalçın, H., Karayığit, A.I., Cicioğlu, E. and Gümüşer, G. (1997) Relationship between clay mineralogy and whole-rock geochemistry of Sorgun (Yozgat) Eocene Coal Basin, Central Anatolia, Turkey. Pp. 15–24 in: *Proceedings of the 8th National Clay Symposium, Kütahya*, Turkey.
- Wesolowski, D.J. (1992) Aluminium speciation and equilibria in aqueous solution: I. Gibbsite solubility in the system Na-K-Cl-OH-Al(OH)₄ from 0 to 100°C. *Geochimica et Cosmochimica Acta*, **56**, 1065–1092.
- Wesolowski, D.J. and Palmer, D.A. (1994) Aluminium speciation and equilibria in aqueous solution: V. Gibbsite solubility at 50°C and pH 3-9 in 0.1 molal NaCl solutions. *Geochimica et Cosmochimica Acta*, **58**, 2947–2970.

(Received 12 June 2000; revised 7 June 2001; Ms. 458)